ARTICLES

Electronic structure of CuV_2S_4

Z. W. Lu and B. M. Klein
Department of Physics, University of California, Davis, California 95616-8677

E. Z. Kurmaev, V. M. Cherkashenko, V. R. Galakhov, S. N. Shamin, Yu. M. Yarmoshenko, and V. A. Trofimova
Institute of Metal Physics, Russian Academy of Sciences–Ural Division, S. Kovalevskaya Street 18, 620219 Yekaterinburg GSP-170, Russia

St. Uhlenbrock and M. Neumann
Universität Osnabrück, Fachbereich Physik, Barbarastrasse 7, D-49069 Osnabrück, Germany

T. Furubayashi
National Research Institute for Metals, 1-2-1 Sengen, Tsukuba 305, Japan

T. Hagino and S. Nagata
Department of Materials Science and Engineering, Muroran Institute of Technology, 27-1 Mizumoto-cho, Muroran 050, Japan
(Received 21 September 1995)

The results of *ab initio* band-structure calculations and measurements of x-ray-emission valence spectra (XES) (Cu $L\alpha$, V $K\beta_5$, V $L\alpha$, S $K\beta_{1,3}$, S $L_{2,3}$) and x-ray-photoelectron valence-band and core-level spectra (XPS) of CuV_2S_4 thiospinel are presented. It is found that a peak in valence-conduction bands close to Fermi level is formed by V $3d$ states, which provide the metallic properties of CuV_2S_4. The valence band is formed by Cu $3d$, V $3d$, V $4p$, and S $3p$ states. Examination of the XES and XPS results and the calculated charge-density maps and densities of states indicates that the valences of both Cu and V are similar to those of their elemental solids. Calculations show a strong electron-phonon coupling in CuV_2S_4 and the prospect of superconducting behavior has not been confirmed.

I. INTRODUCTION

The sulphospinels and selenospinels of CuM_2X_4-type (where $M=$ Ti, V, Cr, Co, Rh, and Ir; $X=$ S, Se, Te) show a variety of structural, electrical, and magnetic properties.[1,2] For instance, a metal-insulator transition was found recently for $CuIr_2S_4$;[3–5] CuV_2S_4 exhibits a phase transition associated with charge-density waves;[6,7] and superconductivity with $T_c = 3.45-4.80$ K was measured for $CuRh_2Se_4$, CuV_2S_4, and $CuRh_2S_4$.[8] However, recent experiments on high-quality single crystals did not confirm superconductivity in CuV_2S_4.[9,10]

Two empirical models of the electronic structure of $CuCr_2X_4$ compounds were suggested to explain their physical properties.[11–16] The first model[11–13] is based on the formula $Cu^+[Cr^{3+}Cr^{4+}]X_4$ with assumptions that diamagnetic Cu^+ ions occupy the tetrahedral sites and that the ferromagnetic moment arises from a parallel alignment of the spins of Cr^{3+} and Cr^{4+} present at the octahedral sites. The metallic conduction and the ferromagnetic interaction are attributed to double exchange between Cr^{3+} and Cr^{4+}. According to the second model,[14–16] the octahedral sites are occupied by Cr^{3+}, and the tetrahedral sites are occupied by formally divalent copper. In this model the metallic conduction and the magnetic behavior are explained by assuming that the $3d$ levels of Cu^{2+} are broadened into an energy band.

In the present paper the results of *ab initio* electronic structure calculations (band structure and density of states) and high-energy spectroscopy measurements of a CuV_2S_4 single crystal, including XPS valence-band and core-level spectra and x-ray-emission valence spectra of each component (Cu $L\alpha$, V $K\beta_5$, V $L\alpha$, S $K\beta_{1,3}$, S $L_{2,3}$), are presented together. This allows us to study the oxidation states of the copper and vanadium ions and to check the above-mentioned models of the electronic structure of thiospinel compounds. We will analyze the bonding feature of CuV_2S_4 in terms of the calculated charge distributions. We also estimate electron-phonon coupling strength and superconductivity using our calculated electronic structure within the McMillan-Hopfield theory.

II. COMPUTATIONAL AND EXPERIMENTAL DETAILS

A. Calculation

We have calculated the band structure and density of states (DOS) of crystalline CuV_2S_4 using the linearized augmented-plane-wave method (LAPW) based on the local-density approximation (LDA),[17] in which we have used the exchange-correlation potential of Ceperley and Alder,[18] as parameterized by Perdew and Zunger.[19] CuV_2S_4 crystallizes

in the face-centered-cubic Al_2MgO_4-type structure (with Pearson symbol of cF56, space group of $Fd3m$ at room temperature. The primitive unit cell contains 14 atoms (two formula units): two Cu atoms occupy the (0,0,0) and $(\frac{1}{4},\frac{1}{4},\frac{1}{4})$ positions, four V atoms occupy the $(\frac{5}{8},\frac{5}{8},\frac{5}{8})$ and equivalent positions, while eight S atoms occupy the (u,u,u) and equivalent positions. We use the experimental lattice parameter[20] of $a=9.799$ Å and $u=0.3807$ in our calculations. In this structural configuration, Cu atoms tetrahedrally coordinate with S atoms, S atom tetrahedrally coordinates with one Cu atom and three V atoms (at a slightly larger distance compared with the Cu-S distance), while V atom coordinates with six S atoms (in the center of an octahedron). The LDA equations are solved self-consistently by the LAPW method.[21,22] The core states are treated fully relativistically, while the valence states are treated semirelativistically (without spin-orbit interaction, which plays a relatively minor role here). No shape approximation is made for either the potential or the charge density. The muffin-tin sphere radii are 1.106, 1.217, and 1.111 Å for Cu, V, and S, respectively. The nonspherical charge density and potential are expanded in terms of lattice harmonics of angular momentum $l\leqslant 8$ inside the muffin-tin spheres and are expanded in more than 14 300 plane waves in the interstitial region. A basis set of about ~100 LAPW's/atom are used. During the self-consistency cycle, the Brillouin zone (BZ) integration is performed using 28 special **k** points[23] in the irreducible BZ. The total DOS and site-decomposed local DOS (LDOS, within the muffin-tin sphere) are calculated using the tetrahedron method[24,25] interpolated from the energy eigenvalues of 195 **k** points directly calculated using the LAPW method. The DOS are smoothed using a Gaussian function with half width of 0.2 eV.

B. Experiment

The x-ray-photoemission spectroscopy (XPS) valence-band and core-level spectra of CuV_2S_4 were measured using an ESCA spectrometer of Perkin-Elmer (PHI 5600 ci, monochromatized Al $K\alpha$ radiation). The single crystal of CuV_2S_4 was cleaved in high vacuum prior to the measurements of the XPS spectra. The XPS spectra were calibrated based on the Au $4f$ spectra of metallic Au ($E_B=$ 84.0 eV).

The Cu $L\alpha$ and V $L\alpha$ ($2p$-$3d4s$ transition) x-ray-emission spectra (XES) were measured on the RSM-500–type x-ray vacuum spectrometer with a diffraction grating ($N=600$ lines/mm; $R=6$ m) and electron excitation. V $L\alpha$ and Cu $L\alpha$ spectra were recorded in the first and second order of reflection, respectively, by a secondary electron multiplier with a CsI photocathode. The energy resolution was about 0.4 eV for V $L\alpha$ XES and 0.55 eV for Cu $L\alpha$ XES. The x-ray tube was operated at $V=4.6$ keV, $I=0.4$ mA.

The V $K\beta_5$ ($1s$-$4p$ transition) and S $K_{1,3}$ ($1s$-$3p$ transition) x-ray-emission spectra were measured using a fluorescent Iohan-type vacuum spectrometer with a position-sensitive detector.[26] Cu K and Pd L x-ray radiation from the special sealed x-ray tubes was used for the excitation of the fluorescent V $K\beta_5$ and S $K_{1,3}$ XES, respectively. A quartz single crystal (1011 plane) curved to $R=2000$ mm (for measurements of V $K\beta_5$ XES) and to $R=1300$ mm (for measurements of S $K_{1,3}$ XES) served as a crystal analyzer. The V $K\beta_5$ and Si $K_{1,3}$ XES were measured with an energy resolution of about 0.35 and 0.25 eV, respectively.

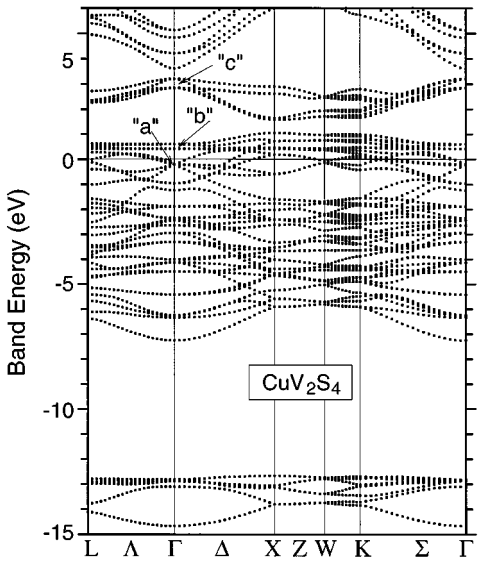

FIG. 1. The calculated band structure of CuV_2S_4 along some high symmetry lines. The Fermi energy is denoted by a solid, thin line at $E=0.0$ eV. The Brillouin zone here is the same as that of an fcc lattice.

The S $L_{2,3}$ x-ray-emission spectrum was studied with the help of small-spot ultrasoft x-ray-emission spectrometer with diffraction grating ($N=600$ lines/mm; $R=2$ m) and electron excitation.[27] S $L_{2,3}$ spectra were measured with an energy resolution of about 0.3 eV. The x-ray tube was operated at $V=5$ keV, $I=130$ nA.

X-ray-emission spectra have been brought to the scale of binding energies with respect to the Fermi level using the binding energies of relevant initial (core-level) states of the x-ray transitions as measured by the XPS technique. Corresponding binding energies are E_B(Cu $2p$)=932.8 eV, E_B(V $2p$)=513.5 eV, E_B(S $2p$)=161.0 eV. The values of E(V $K\alpha_1$)=4952.2 eV and E(S $K\alpha_1$)=2307.6 eV were taken for comparison with the V $L\alpha$ and V $K\beta_5$ XES and S $K\beta_{1,3}$ XES.

The CuV_2S_4 single crystal was synthesized in a quartz ampoule by $TeCl_4$ vapor transport at growth temperatures from 830 to 720 °C in a two-zone furnace. The crystals grow as octahedrons with a maximum size about $3\times3\times3$ mm^3. According to the x-ray-diffraction pattern, the pure spinel phase is obtained. The characterization of the crystals and the results of measurements of some electrical and magnetic properties are given in Ref. 10.

III. RESULTS

A. Calculation

Figure 1 depicts the calculated band structure of CuV_2S_4 along some high-symmetry lines. The S $3s$-derived bands located from ~−15 to −13 eV below the Fermi energy (denoted by a thin, solid line at $E=0$ eV) are well separated from the rest of the valence bands by more than ~5 eV. The S $3s$ bands are quite narrow except for the lowest two bands (at ~−14 eV) with widths of ~0.6 eV,

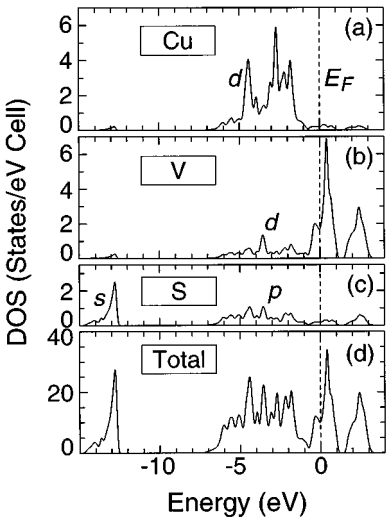

FIG. 2. The calculated total and site-decomposed density of states for CuV_2S_4 (a) Cu LDOS, (b) V LDOS, (c) S LDOS, and (d) total DOS. The Fermi energy is denoted by dashed lines at $E=0.0$ eV. The major character of these states are indicated by s, p, d. See Fig. 5 for further detail.

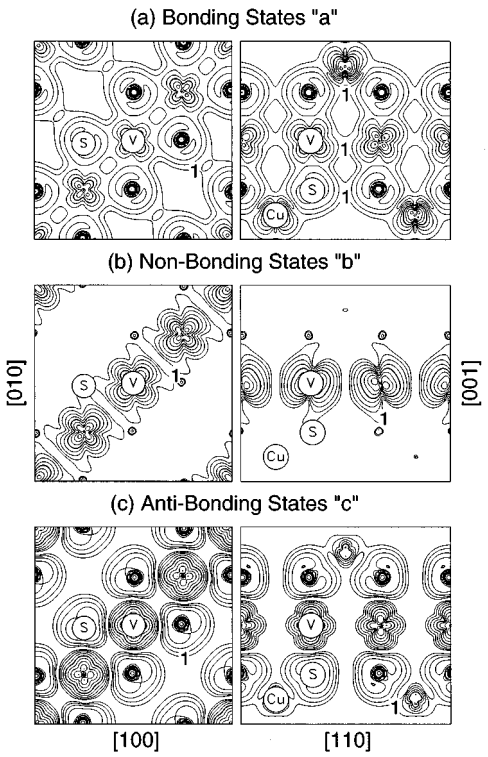

FIG. 3. Charge distributions in the (001) (left panels) and $(1\bar{1}0)$ (right panels) planes for various states (a, b, and c shown in Fig. 1) at the zone center, Γ point: (a) the bonding states a from -0.22 to -0.19 eV, (b) nonbonding and antibonding states b from 0.42 to 0.62 eV, and (c) the antibonding states c from 2.84 to 3.21 eV. Note that the $(1\bar{1}0)$ plane contains the Cu, V, and S atoms, and the (001) plane contains the V atoms, while S atoms are slightly off the (001) plane. The successive contour levels differ by $\rho_{n+1}/\rho_n=2.226$. The lowest contour levels are labeled in the figure (in the units of 0.01 e/Å^3). Note that in (b) the charges are localized around the V atoms with a node between the V-V bond (antibonding), and in (c) there are nodes between V-V, V-S, and S-S bonds.

while width between the lowest s band and highest s bands (threefold degenerate) at the Γ point is 1.84 eV. The band manifolds in the energy region of ~ -7 eV below the Fermi level are derived mainly from the Cu $3d$, V $3d$, and S $3p$ states. The bands near the Fermi energy are predominantly of V $3d$ character, so that the metallic nature of CuV_2S_4 comes mainly from the V atom. The bands immediately above the Fermi energy are rather flat, which leads to a sharp peak in the density of states just above E_F, as shown in Fig. 2. One also notices that there appears a band gap of 0.2 eV at $E\sim 1$ eV above the Fermi energy, separating the predominant t_{2g} and e_g bands of V, which has a local octahedral symmetry. As seen in Fig. 2, the Cu d-band manifold is nearly exclusive to the range -7 to -1 eV below E_F.

Figure 3 shows the charge distributions in the (100) and $(1\bar{1}0)$ planes for the states a, b, and c at the zone-center Γ point as indicated in Fig. 1. The six states a are just below the Fermi energy (from -0.22 to -0.19 eV). Figure 3(a) shows that these are the bonding states, as the S lobes strongly orient towards nearest-neighbor Cu and V atoms. However, the V atoms exhibit t_2 (d_{xy}, d_{yz}, and d_{zx}) types of orbitals with lobes pointing towards other V atoms rather than towards nearest-neighbor S atoms. On the other hand, the six states b immediately above the Fermi energy (from 0.42 to 0.62 eV) are nearly pure V d_{xy}, d_{yz}, and V d_{zx} orbitals with little weight on the Cu or S sites as shown in Fig. 3(b). Note that the unoccupied bands along the Λ axis (L to Γ) are nearly dispersionless. We also notice that there is a node between the V-V bonds (best seen on a line plot, however, not shown here), indicating V-V antibonding character. The upper e_g complex is made up of V-d and S-p hybridized antibonding bands. Examining the charge distribution associated with the eight states c, $\sim$ 2 eV above the states b one clearly observes the hybridized V-e_g and S-p antibonding nature, as there are nodes along the V-S and Cu-S bonds [Fig. 3(c)]. The charge distribution clearly exhibits the $d_{x^2-y^2}$ and d_{z^2} character on the V atoms, while the S lobes orient away from the nearest Cu and V neighbors.

Figure 4 depicts the valence charge density (excluding the S $3s$ states at ~ -13 to -15 eV) and difference charge-density (total charge density with respect to an overlapping atomic charge density). Besides the expected ionic bonding character based on the elemental electronic configurations, one clearly sees covalent and metallic features as well, i.e., the S-p lobes orient toward the nearest neighbor Cu and V in Fig. 4(a) and charge piles up on the Cu-S and V-S bonds in Fig. 4(b). Note that the valence charge density is almost spherical around the Cu atoms and the difference charge-density map shows only slightly directional bonding around Cu (unlike around the V atom), indicating a nearly full d^{10} shell, as can be surmised from the DOS shown in Figs. 2 and 5.

The band structures of spinel CuM_2S_4 ($M=$ Co, Rh, and Ir) have been recently reported by Oda *et al.*[28] and are fairly similar to our calculated bands of CuV_2S_4. The presence of the t_{2g} and e_g band gap is also seen[28] in the CuM_2S_4 ($M=$ Co, Rh, and Ir) materials.

Figure 2 shows the full DOS and several of the site-decomposed local DOS (LDOS) of CuV_2S_4. One immedi-

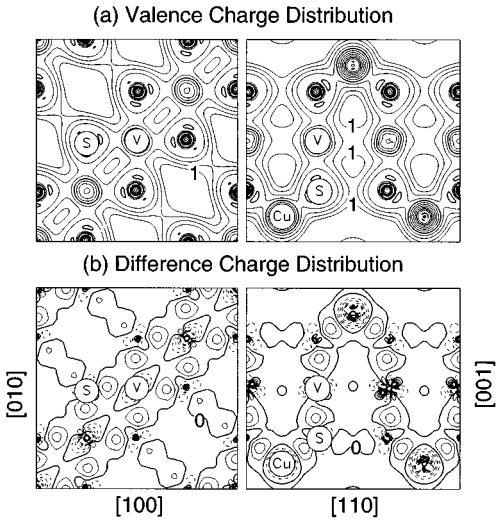

FIG. 4. Calculated (a) valence (excluding the S 3*s* states) and (b) difference charge-density distribution (total charge density with respect to the overlapping atomic charge density, $\Delta\rho=\rho_{\text{total}}-\rho_{\text{atom}}$) for CuV_2S_4 in the $(00\underline{1})$ (left panels) and $(1\bar{1}0)$ (right panels) planes. Note that the $(1\bar{1}0)$ contains the Cu, V, and S atoms and (001) plane contains the V atoms, while S atoms are slightly off the (001) plane. The successive contour levels in (a) differ by $\rho_{n+1}/\rho_n=1.649$. The lowest contour levels are labeled in the figure (in the units of 0.1 e/Å^3), while in (b) the contour levels differ by $\Delta\rho_{n+1}-\Delta\rho_n=0.05$ e/Å^3. The thick solid contour next to the dashed line denote $\Delta\rho=0.00$ contour.

ately notices that the Fermi energy is located in a dip of the DOS. It has been previously observed from first-principles calculations that the stable structures tend to adopt a structure which has a small density of states at the Fermi energy.[29–32] The DOS features immediately below and above the Fermi energy (from -1 eV to 3 eV) consist of mainly V 3*d* states. In the bonding region of (-5.0 eV to -1.5 eV below Fermi energy) Cu 3*d* DOS dominates, while S 3*p* and V 3*d* contribute substantially in this region as well. These can be seen clearly from Fig. 5, which gives the *s*, *p*, and *d* site-decomposed and angular-momenta-decomposed DOS for Cu, V, and S. The *s* and *p* LDOS of Cu and V are approximately a factor of 10 smaller than the corresponding *s* and *p* LDOS of S, while the S 3*d* DOS is negligible.

B. Comparison of experiment and calculation

To compare our calculated electronic-structure results with the experimental XPS and XES spectra, we have made use of our calculated DOS results with the neglect of energy-dependent matrix-element effects. The replacement of the matrix elements by a constant should only affect the comparisons of the absolute intensities since the former are generally smooth functions of energy. For the XPS spectra comparisons we use the total DOS, while for comparison with the *K* and *L* spectra for the constituent elements we use the *p* and *d* DOS, respectively (we comment on the *s*-like contributions in the discussion below).

XPS and XES valence-band spectra along with a comparison with the calculated DOS are shown in Fig. 6. We see that there is fairly good agreement between experiment and theory, except for a more or less rigid shift of ~ 1 eV in the upper valence-band region. Experimentally, one sees that the high-energy shoulder of the XPS valence-band spectrum near E_F is close to the high-energy subband of the V $L\alpha$ XES. This confirms the theoretical conclusion that the metallic properties of CuV_2S_4 are governed by the V 3*d* electron states. The most intensive subband of the XPS valence-band spectrum is located at -3 eV and is due to Cu 3*d* states (also seen in the calculated total DOS). This conclusion can be inferred from the large photoionization cross sections of Cu 3*d* states with respect to those of V 3*d*, S 3*s*, and S 3*p* states, and is also verified by the coincidence of the location of the intensity maximum in the XPS spectrum with that of the intensity maximum of the Cu $L\alpha$ XES. This interpretation is also confirmed by the special measurements of the XPS valence-band spectrum of CuV_2S_4 after ion sputtering of the surface, which showed a decrease of intensity of this peak due to the decrease of the Cu concentration (see Fig. 7). Note that the states above the Fermi level (sputtered crystal) are due to a defect pinning. The defects are caused by the sputtering procedure.[33] It is the additional evidence for the interpretation of XPS VB spectrum of CuV_2S_4. The next low-intensity shoulder of the XPS VB spectrum at *E* about -5 eV is connected with the S 3*p*–Cu 3*d*–V 3*d*–V 4*p* hybridized subbands which can be seen from the closeness of the energy position of the intensity maxima of the S $K\beta_{1,3}$, Cu $L\alpha$ (low-energy subband), V $L\alpha$ (low-energy subband), and V $K\beta_5$ x-ray-emission spectra and from the calculated LDOS. The low-energy peak of the XPS valence-band spectrum of CuV_2S_4 located at $E\sim -14$ eV is formed by predominantly S atomiclike 3*s* states mixed with a very small amount of *s* and *p* states of Cu and V. The fact that the DOS peak is approximately 2 eV higher in energy than the experiment is probably due to error in the LDA.

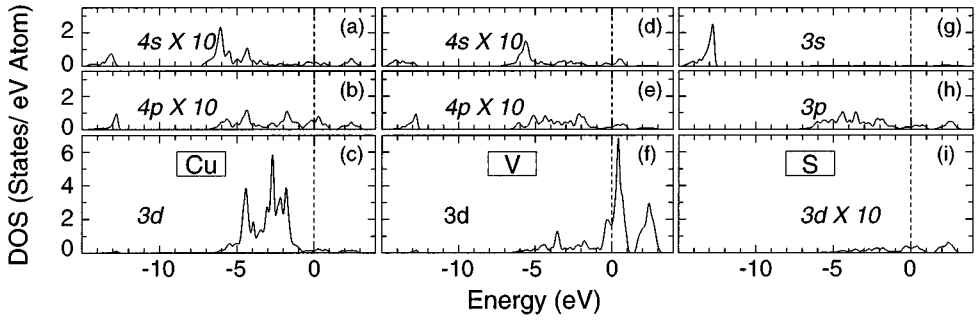

FIG. 5. Site-decomposed and angular-momenta-decomposed density of states for CuV_2S_4: (a) Cu *s*, (b) Cu *p*, (c) Cu *d*, (d) V *s*, (e) V *p*, (f) V *d*, (g) S *s*, (h) S *p*, (i) S *d* LDOS. Note that some of the LDOS's have been multiplied by a factor of 10. The Fermi energy is denoted by dashed lines at $E=0.0$ eV.

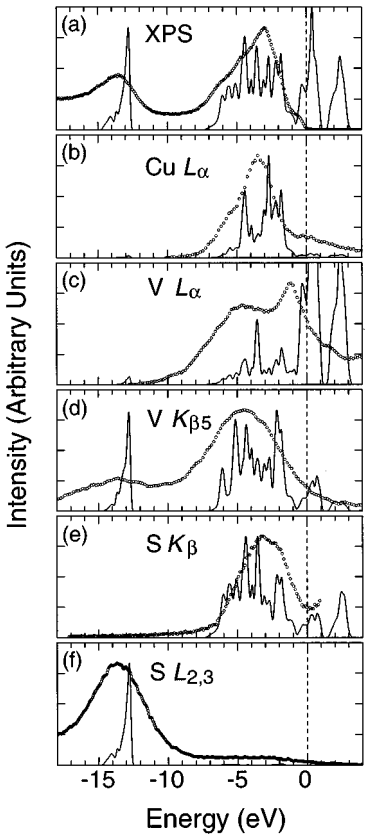

FIG. 6. Comparison between (a) calculated total DOS and measured XPS spectra, (b) Cu d LDOS versus Cu $L\alpha$ XES spectra, (c) V d LDOS versus V $L\alpha$ XES spectra, (d) V p LDOS versus V $K\beta5$ XES spectra, (e) S p LDOS versus S $K\beta$ XES spectra, and (f) S s LDOS versus S $L_{2,3}$ XES spectra. To facilitate the comparison, we renormalize both data sets such that their respective maxima (at E less than the Fermi energy) correspond to the same value. The Fermi energy is denoted by dashed lines.

One of the most intriguing question for analysis of electronic structure of the CuV_2S_4 thiospinel is connected with the determination of the oxidation states of the copper and vanadium atoms (or the formal valence counts). According to our XPS measurement shown in Fig. 7, the Cu $2p$ binding energy of CuV_2S_4 is closer to that of Cu and Cu $_2$O than to that of CuO.[34] Therefore, one can conclude from this measurement that the oxidation state of Cu atoms of this compound is closer to Cu^+. A characteristic feature of XPS $2p$ spectra of Cu-containing compounds that would provide evidence in favor of a Cu^{2+} oxidation state is a high-energy satellite structure that is found for CuO and all high-T_c superconducting cuprates.[34,35] As seen from Fig. 8, this structure is not found in the XPS Cu $2p$ spectra of CuV_2S_4. Another spectral test for the determination of the oxidation state of Cu atoms in compounds is connected with measurements of the ratio of spectral and integrated intensities of Cu $L\beta$ ($2p_{1/2}$-$3d4s$ transition) and Cu $L\alpha$ ($2p_{3/2}$-$3d4s$ transition) x-ray-emission spectra. According to Ref. 36, the ratio of integrated intensities I(Cu $L\beta$)/I(Cu $L\alpha$) for Cu_2O and CuO is 0.18 and 0.26, respectively. According to our measurements (Fig. 8), this ratio for CuV_2S_4 is about 0.21, which is closer to Cu_2O than to CuO.

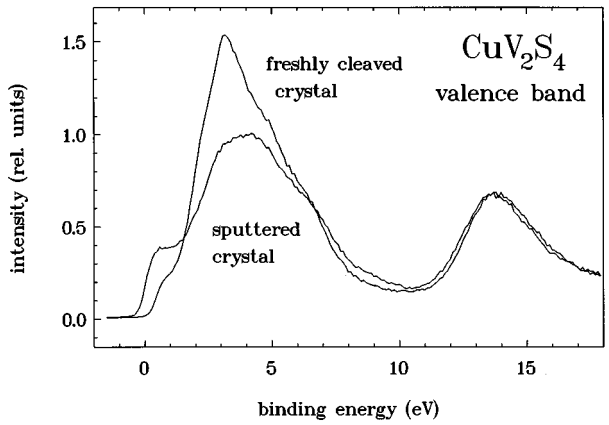

FIG. 7. Measured valence-band spectra of CuV_2S_4 for a freshly cleaved crystal and a sputtered crystal. The states above the Fermi level for the sputtered crystal are due to a defect pinning. The defects are caused by the sputtering procedure. Note that after the ion sputtering, the intensity of the Cu $L\alpha$ peak decreases.

The oxidation state of vanadium atoms of CuV_2S_4 can also be estimated from XPS and XES measurements. In the case of XPS it is rather difficult because of the absence of good-quality single crystals of reference compounds. The V $L\alpha$ x-ray-emission band shows a splitting for two subbands and a ratio of low-energy and high-energy subbands is also sensitive to oxidation state of vanadium in compounds. According to Ref. 37, this ratio is about 0.75 and 1.0 for V_2O_3 and VO_2, respectively. We have found that for CuV_2S_4 is about 0.8, i.e., closer to that of V_2O_3.

Theoretically, it is impossible to unambiguously assign charge to a particular atom (or site) in a solid, since the orbitals overlap and hybridize with each other. Formal valence count is only well defined for ionic crystals such as NaCl, where the Na (Cl) ion loses (gains) approximately one electron (Na^+ and Cl^{-1}). In such ionic materials, the charge state of the ions can be seen by comparing the self-consistent charge densities and energy bands with those obtained from overlapping ionic charge densities without the self-consistent loop. For CuV_2S_4, a system with substantial covalent and metallic bonding (see Fig. 4), the formal valence is less meaningful. Table I gives atomic site and angular-momentum decomposed charges within the muffin-tin

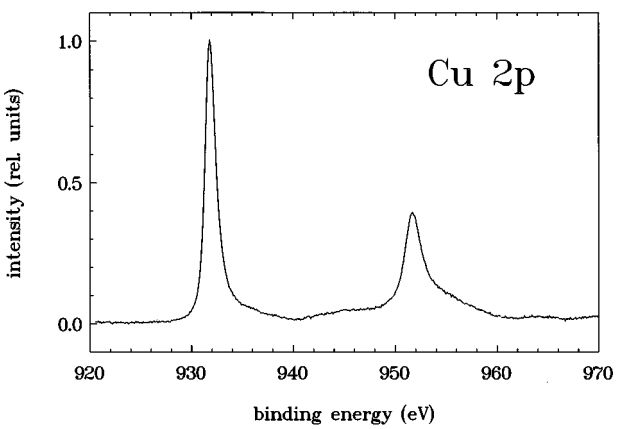

FIG. 8. Measured Cu (in CuV_2S_4) XPS $2p$ core spectra.

TABLE I. Angular momentum and atomic site-decomposed charge (in units of the electronic charge e) inside the muffin-tin spheres (R_{MT} is the muffin-tin radii). For comparison, we also give the charge of elemental fcc Cu and bcc V in their respective experimental lattice constants.

	Cu (R_{MT}=1.106 Å)		V (R_{MT}=1.217 Å)		S (R_{MT}=1.111 Å)
	Compound	Element	Compound	Element	
$Q(s)$	0.331	0.344	0.222	0.294	1.456
$Q(p)$	0.308	0.262	0.293	0.276	2.715
$Q(d)$	9.007	8.983	2.890	2.946	0.085
Q(tot)	9.665	9.600	3.448	3.533	4.266

spheres in the CuV_2S_4 compound and in elemental fcc Cu and bcc V. Interestingly, the calculated total charge within the Cu muffin-tin sphere for the compound is slightly larger than in the elemental fcc Cu, while the opposite is true for V. Note that the Cu and V p-electron counts in the compound are larger than in their elemental solid, which can be explained by noticing that the p orbitals of S are fairly extended, much of the charge is outside its muffin-tin sphere, and is subsequently counted as Cu and V p electrons. Note that the Cu-S (2.218 Å) and V-S (2.395 Å) bond lengths are much smaller than the Cu-Cu (2.553 Å) and V-V (2.624 Å) bond lengths in their respective equilibrium elemental solid.

The Cu and V $3d$ orbitals are more localized than their $4s$ and $4p$ orbitals, and d-electron charge will be mostly included in the muffin-tin spheres. Hence, the d-electron occupation of Cu and V will reflect their valence states more reliably than their total electron count. Cu^+ and Cu^{2+} will have d^{10} and d^9 configurations, respectively, while V^{2+}, V^{3+}, and V^{4+} will have d^3, d^2, and d^1 configurations, respectively. Table I shows that within the muffin-tin spheres there are 9.0 d electrons for Cu (the isolated atom has 10 d electrons in all space), 2.9 d electrons for V (the isolated atom has 3 d electrons in all space), and only 2.7 p electrons for (the isolated atom has 4 p electrons in all space). From the present calculations, it is unlikely that the valence count for V is 4+, it is between 2+ and 3+, while for Cu a valence count will be between 1+ and 2+. Since the Cu d count is only slightly larger in CuV_2S_4 than in pure Cu, the Cu valence in CuV_2S_4 is closer to 1+ than to 2+. Examining the valence and difference charge-density distribution (Fig. 4), one sees a nearly spherical charge distribution rather than directional distribution, indicating an almost fully occupied d band (d^{10} configuration) or Cu^+ instead of a d^9 configuration or Cu^{2+}. Furthermore, the Cu d-like DOS is very similar to that of Cu metal with a filled d band. Therefore, our electronic structure results lead to the same conclusion obtained from a study of the XPS and XES experimental results: the valence of Cu is close to Cu^+. In addition, we conclude that the valence of V is close to its metallic valence state.

C. Electron-phonon couplings and superconductivity

We estimate the electron-phonon coupling strengths (the McMillan-Hopfield parameters η) for each atom in the unit cell in the CuV_2S_4 system utilizing the Gaspari and Gyorffy[38,39] rigid-muffin-tin approximation (RMTA), an approach that is known to work reasonably well for metals, although there are some caveats for this system that we will discuss. Furthermore, estimates of the superconducting transition temperature T_c can be made using a Debye-like model for the phonon spectrum. This is a further approximation on top of the RMTA, but is the best estimate we can make for T_c lacking either experimental or calculated values for the phonon spectrum other than estimates of the Debye temperature from specific-heat measurements.

The electronic structure inputs into the RMTA are the muffin-tin-ized potentials of each component and the total and site-angular-momentum-decomposed densities of states, all available from our calculations. The calculated η values are given in Table II, where the values per site are shown as well as the unit-cell contributions, and the values of η for elemental Cu and V (elemental S, being nonmetallic, has not been calculated), obtained from Ref. 40, are also shown.

The full unit-cell value of η=3.08 eV/Å^2 for CuV_2S_4 is substantial, with relatively large contributions from the V and S sites. A semiquantitative estimate of the superconducting transition temperature for this system can be obtained if one uses for the phonon factor in λ, the mass enhancement factor, the Debye temperature of approximately Θ_D=200 K estimated from the experiments of Hagino *et al.*[10] (obtained from the specific-heat measurements), yielding $\lambda_{e-p}\sim 2.0$. Inputting this into the McMillan equation for T_c, one obtains a value of approximately 20 K for the transition temperature (using $\mu^*=0.13$).

Hagino *et al.* also extrapolate their specific-heat measurements to obtain an electronic specific-heat γ_{exp} value of 50 mJ/K^2 mol. Our calculated density of states at the Fermi energy of $N(E_F)$=96.8 states/Ry unit cell (one unit cell has two CuV_2S_4 molecules) leads to $\gamma_{th}=\frac{1}{3}\pi^2 k_B^2 N(E_F)$=8.38 mJ/K^2 mol. This would give a large $\lambda_{tot}=\gamma_{exp}/\gamma_{th}-1$ value of 4.97, which is more than twice the value estimated from

TABLE II. The McMillan-Hopfield electron-phonon parameters, η_a, for the atom components of CuV_2S_4 in units of eV/Å^2. For the compound, both the individual site components are shown, as well as the full unit-cell contributions in parentheses (there are 2, 4, and 8 atoms of Cu, V, and S, respectively). The values for the monoatomic elements Cu and V are shown in the last column (from Ref. 40) for comparison.

Element	η_a CuV_2S_4 compound	η_a Pure metals
Cu	0.009 (0.018)	0.456
V	0.539 (2.156)	6.894
S	0.113 (0.904)	not available

the electron-phonon interaction. Note that the calculated Fermi energy is located in a dip of a sharply rising feature in the DOS, so that moving our calculated Fermi energy up by 0.05 eV would nearly double our calculated N_F, and hence double the γ_{th} value as well, which in turn would give a λ_{tot} value comparable to λ_{e-p}. One also notices that γ_{exp} value of CuV_2S_4 is rather large, twice as large as the similar spinel compound $CuRh_2S_4$,[41] which is a superconductor with $T_c \sim 4$ K.

Hagino *et al.*[10] claim that there is no indication of superconductivity in a single crystalline sample of CuV_2S_4, despite earlier claims of superconductivity for powdered samples. Although the RMTA is expected to be of only-semiquantitative accuracy for the complex crystal structure of CuV_2S_4, it is clear that theory predicts respectable superconductivity for this system, in disagreement with experiment, if the use of Debye approximation is a reasonable approximation to the true coupling with the phonons. In addition, the specific-heat-derived λ_{tot} also indicates relatively high T_c for this system.

The discrepancy between theory and experiment regarding superconductivity in CuV_2S_4 is large and disturbing. The unusual specific-heat-derived values of λ and θ_D indicate unusual properties of this compound that warrant further investigation, both theoretical and experimental.

IV. CONCLUSIONS

We have presented experimental XPS and XES measurements for the thiospinel compound CuV_2S_4 and compared the results to *ab initio* electronic structure calculations of the band structure-derived densities of states. Good agreement has been found between theory and experiment as to the energy-dependent structure seen in the experiments. An analysis of the XPS and XES experiments and the theoretical charge densities shows that Cu is in a metalliclike valence state with approximately 10 *d* electrons in occupied states, with a similar conclusion for a metalliclike valence of V in this compound. The calculated charge density also confirms this interpretation. From our electronic structure results and the Debye temperature determined from specific-heat measurements, we have also estimated the electron-phonon coupling strength in CuV_2S_4 and find a large λ value of ~ 2.0 and the prediction of robust superconductivity in CuV_2S_4. The λ value extracted from the specific-heat measurements using our calculated $N(E_F)$ is even larger and would lead to an even larger T_c. It is puzzling that the same crystals on which the specific heat measurements were made shows no indication of superconductivity. Further studies of the CuV_2S_4 system are called for.

[1] R. J. Bouchard, P. A. Russo, and A. Wold, Inorg. Chem. **4**, 685 (1965).

[2] M. Robbins, P. K. Baltzer, and E. Lopatin, J. Appl. Phys. **39**, 662 (1968).

[3] S. Nagata, T. Hagino, Y. Seki, and T. Bitoh, Physica B **194-195**, 1077 (1994).

[4] T. Furubayashi, T. Matsumoto, T. Hagino, and S. Nagata, J. Phys. Soc. Jpn. **63**, 3333 (1994).

[5] T. Hagino, T. Tojo, T. Atake, and S. Nagata, Philos. Mag. B **71**, 881 (1995).

[6] T. Sekine, K. Uchinokura, H. Iimura, R. Yoshizaki, and E. Matsuura, Solid State Commun. **51**, 187 (1984).

[7] J. Mahy, D. Colatis, D. Van Dyck, and S. Amelinck, J. Solid State Chem. **68**, 320 (1987).

[8] N. H. Van Maaren, G. M. Schaeffer, and F. K. Lotgering, Phys. Lett. **25A**, 238 (1967).

[9] Y. Seki, T. Hagino, S. Takayanagi, and S. Nagata, J. Phys. Soc. Jpn. **61**, 2597 (1992).

[10] T. Hagino, Y. Seki, S. Takayanagi, N. Wada, and S. Nagata, Phys. Rev. B **49**, 6822 (1994).

[11] F. K. Lotgering, *Proceedings of the International Conference on Magnetism, Nottingham* (Institute of Physics and Physical Society, London, 1964), p. 533.

[12] F. K. Lotgering and R. P. van Stapele, Solid State Commun. **5**, 143 (1967).

[13] F. K. Lotgering and R. P. van Stapele, J. Appl. Phys. **39**, 417 (1968).

[14] J. B. Goodenough (unpublished).

[15] J. B. Goodenough, Solid State Commun. **5**, 537 (1967).

[16] J. B. Goodenough, J. Phys. Chem. Solids **30**, 261 (1969).

[17] P. Hohenberg and W. Kohn, Phys. Rev. **136**, B864 (1964); W. Kohn and L. J. Sham, *ibid.* **140**, A1133 (1965).

[18] D. M. Ceperley and B. J. Alder, Phys. Rev. Lett. **45**, 566 (1980).

[19] J. P. Perdew and A. Zunger, Phys. Rev. B **23**, 5048 (1981).

[20] P. Villiar and L. D. Calvert, *Pearson's Handbook of Crystallographic Data for Intermetallic Phases* (ASM International, Materials Park, OH, 1991), Vol. 3, p. 2977.

[21] O. K. Andersen, Phys. Rev. B **12**, 3060 (1975); E. Wimmer, H. Krakauer, M. Weinert, and A. J. Freeman, *ibid.* **24**, 864 (1981); D. R. Hamann, Phys. Rev. Lett. **42**, 662 (1979); S.-H. Wei and H. Krakauer, *ibid.* **55**, 1200 (1985); S.-H. Wei, H. Krakauer, and M. Weinert, Phys. Rev. B **32**, 7792 (1985).

[22] D. J. Singh, *Planewaves, Pseudopotentials, and the LAPW Method* (Kluwer, Boston, 1994).

[23] H. J. Monkhorst and J. D. Pack, Phys. Rev. B **13**, 5188 (1976).

[24] G. Lehmann, P. Rennert, M. Taut, and H. Wonn, Phys. Status Solidi **37**, K27 (1970); G. Lehmann and M. Taut, *ibid.* **54**, 469 (1972).

[25] O. Jepsen and O. K. Andersen, Solid State Commun. **9**, 1763 (1971).

[26] V. E. Dolgih, V. M. Cherkashenko, E. Z. Kurmaev, D. A. Goganov, E. K. Ovchinnikov, and Yu. M. Yarmoshenko, Nucl. Instrum. Methods Phys. Res. Sect. A **224**, 117 (1984).

[27] E. Z. Kurmaev, V. V. Fedorenko, S. N. Shamin, G. Wiech, and Y. Kim, Phys. Scr. **T41**, 288 (1992).

[28] T. Oda, M. Shirai, N. Suzuki, and K. Motizuki, J. Phys. Condens. Matter **7**, 4433 (1995).

[29] D. M. Nicholson *et al.*, in *High Temperature Ordered Intermetallic Alloys III*, edited by C.T. Liu, A.I. Taub, N.S. Stoloff, and C.C. Koch, MRS Symposia Proceedings No. 133 (Materials Research Society, Pittsburgh, 1989), p. 17; and in *Alloy Phase Stability and Design*, edited by G.M. Stocks, D.P. Pope, and A.F.

Giamei, MRS Symposia Proceedings No. 186 (Materials Research Society, Pittsburgh, 1991), p. 229.
[30] A. E. Carlson and P. J. Meschter, J. Mater. Res. **4**, 1060 (1989).
[31] Jian-hua Xu and A. J. Freeman, Phys. Rev. B **40**, 11 927 (1989); J. Mater. Res. **6**, 1188 (1991).
[32] Z. W. Lu, B. M. Klein, and A. Zunger, Phys. Rev. Lett **75**, 1320 (1995).
[33] H. Kuhlenbeck, G. Odörfer, R. Jaeger, G. Illing, M. Menges, Th. Mull, H.-J. Freund, M. Pöhlchen, V. Staemmler, S. Witzel, C. Scharfschwerdt, K. Wennemann, T. Liedtke, and M. Neumann, Phys. Rev. B. **43**, 1969 (1991).
[34] P. Steiner, V. Kinsinger, I. Sander, B. Siegwart, S. Hüfner, C. Politis, R. Hoppe, and H. P. Müller, Z. Phys. B **67**, 497 (1987).
[35] S. Hüfner, P. Steiner, M. Weirich, and R. Courths, Z. Phys. B **85**, 43 (1991).
[36] S. M. Butorin, V. R. Galakhov, E. Z. Kurmaev, and V. I. Glazyrina, Solid State Commun. **81**, 1003 (1992).
[37] E. Z. Kurmaev, V. M. Cherkashenko, and L. D. Finkelstein, *X-Ray Spectra of Solids* (Nauka, Moscow, 1988).
[38] G. D. Gaspari and B. L. Gyorffy, Phys. Rev. Lett. **29**, 801 (1972).
[39] B. M. Klein and W. E. Pickett, in *Superconductivity in d- and f-Band Metals 1982*, edited by W. Buckel and W. Weber (Kernforschungszentrum Karlsruhe GmbH, Karlsruhe, 1982), p. 477.
[40] D. A. Papaconstantopoulos *et al.*, Phys. Rev. B **15**, 4221 (1977).
[41] T. Hagino, Y. Seki, N. Wada, S. Tsuji, T. Shirane, K. Kumagai, and S. Nagata, Phys. Rev. B **51**, 12 673 (1995).